# Sequential NMR Resonance Assignment and Secondary Structure of Ferrocytochrome $c_{553}$ from *Desulfovibrio vulgaris* Hildenborough†

Dominique Marion*,‡ and Françoise Guerlesquin§

*Institut de Biologie Structurale, CNRS–CEA, 41 Avenue des Martyrs, 38027 Grenoble Cedex 1, France, and Laboratoire de Chimie Bactérienne, CNRS, BP 71-13277 Marseille Cedex, France*

*Received March 11, 1992; Revised Manuscript Received June 1, 1992*

ABSTRACT: Two-dimensional nuclear magnetic resonance spectroscopy was used to assign the proton resonances of ferrocytochrome $c_{553}$ from *Desulfovibrio vulgaris* Hildenbourough at 37 °C and pH = 5.9. Only a few side-chain protons were not identified because of degeneracy or overlap. The spin systems of the 79 amino acids were identified by DQF-COSY and HOHAHA spectra in $H_2O$ and $D_2O$. Sequential assignments were obtained from NOESY connectivities between adjacent amide, $C^{\alpha}H$, and $C^{\beta}H$ protons. From sequential NH($i$) → NH($i$+1) and long-range $C^{\alpha}H(i)$ → NH($i$+3) connectivities, four stretches of helices were identified (2→8, 34→46, 53→59, 67→77). Long-range NOE between residues in three different helices provide qualitative information on the tertiary structure, in agreement with the general folding pattern of cytochrome *c*. The heme protons, including the propionate groups, were assigned, and the identification of Met 57 as sixth heme ligand was established. The dynamical behavior of the ring protons of the six tyrosines was analyzed in detail in terms of steric hindrance. The NMR data for ferrocytochrome $c_{553}$ are consistent with the X-ray structure for the homologous cytochrome from *D. vulgaris* Miyazaki. On the basis of the secondary structure element and of observed chemical shift due to the heme ring current, a structural alignment of eukaryotic and prokaryotic cytochromes *c* is proposed.

Cytochromes *c* form a diverse group of proteins sharing only few features in common. They are found in nearly all forms of life ranging from bacteria, protozoa, and yeast to all higher organisms. Most cytochromes are involved in energy transduction for producing ATP from the oxidation of metabolites or by photosynthesis (Mathews, 1985).

The mitochondrial type of cytochrome *c* is found in a wide variety of eukaryotic and prokaryotic organisms (Dickerson & Timkovich, 1975). The sequences are extremely variable, with the strictly conserved residues located in the heme (iron porphyrin) binding fragment (Dickerson, 1980). In all cases, the sequence Cys-Xxx-Xxx-Cys-His occurs near the N-terminal end whereas the Met ligand is near the C-terminus. The heme group is covalently bound to two cysteine residues by thioether linkages, and the fifth and sixth iron (axial) ligands are ring nitrogen of histidine and sulfur of methionine. Atomic structures, as determined from X-ray crystallography of more than nine respiratory and photosynthetic cytochromes *c*, reveal a common folding pattern for some segments of the polypeptidic chain despite large differences in primary sequence (Chothia & Lesk, 1985).

Recently, an NMR-based comparison of prokaryotic and eukaryotic cytochromes has been performed by Chau et al. (1990). In this study, it was shown that the benzoid rings of Phe and Tyr in cytochrome $c_{551}$ of *Pseudomonas aeruginosa* are rapidly flipping on the NMR time scale in contrast to the larger eukaryotic cytochromes (>100 residues) for which many of them are slowly flipping on the NMR time scale. Thus, in addition to the structural information also available from X-ray data, NMR provides insight into the dynamical behavior of cytochromes *c*, particularly for aromatic side chains. More recently, Detlefsen et al. (1991) have reported the refined 3D structure of this cytochrome $c_{551}$ based on NMR data.

*P. aeruginosa* cytochrome $c_{551}$ is markedly different from mitochondrial cytochrome *c* in various respects: a smaller polypeptidic chain (MW ≈ 9000 versus MW ≈ 13 000) and a modified heme electron distribution due to a different geometry of the methionine ligand (*S* chirality instead of *R* chirality) (Senn & Wüthrich, 1985). Despite these major differences, the redox potential of both proteins is not modified (≈+260 mV).

Dayhoff and Barker (1976) have proposed a phylogenetic tree for the cytochrome *c* superfamily based on primary sequences. Within this superfamily, cytochromes $c_{553}$ from *Desulfovibrio vulgaris* Hildenborough (van Rooijen et al., 1989) and *D. vulgaris* Miyazaki (Nakano et al., 1983) are close relatives of cytochrome $c_{551}$ from *P. aeruginosa*. Furthermore, the *D. vulgaris* cytochrome $c_{553}$ is one of the most primitive members of the cytochrome *c* superfamily known.

The cytochrome $c_{553}$ from the sulfate-reducing bacterium *D. vulgaris* Hildenborough (MW ≈ 9000) is of interest because of its peculiar redox potential (≈10 mV) (Bianco et al., 1983; Bertrand et al., 1982). In addition, Senn et al. (1983) have shown that a rather large conformational change occurs between the oxidized and the reduced forms of this protein. For example, the NMR experiments suggest an *S* chirality for the methionine ligand in the reduced form as opposed to the *R* chirality in the oxidized form indicated by CD Cotton effect at 695 nm. Interestingly, *D. vulgaris* cytochrome $c_{553}$ is the only known example of such a change in chirality, which might be correlated to its peculiar redox potential. The physiological function of this cytochrome is still poorly characterized. However, the cloning and sequencing of the gene encoding for *D. vulgaris* Hildenborough cytochrome $c_{553}$ have provided evidence for its cellular location in the periplasm, which gives some implication for its function. For example,

† This work has been supported by the Centre National de la Recherche Scientifique (Interdisciplinary Program for Protein Engineering IMA-BIO) and the Commissariat à l'Energie Atomique (Department of Life Sciences DSV).

* To whom correspondence should be addressed.
‡ Institut de Biologie Structurale, CNRS–CEA.
§ Laboratoire de Chimie Bactérienne, CNRS.

0006-2960/92/0431-8171$03.00/0 © 1992 American Chemical Society

the cytochrome $c_{553}$ of a closely related strain *D. vulgaris* Miyazaki has been assigned as electron partner for the formate and lactate dehydrogenases (Yagi et al., 1979; Ogata et al., 1981), which are either periplasmic or membrane-bound proteins.

It is anticipated that investigation of the structure and dynamics of cytochrome $c_{553}$ will provide a better understanding on how the respiratory chain has evolved from sulfate respiration in primitive organisms to oxygen respiration in higher species. Preliminary crystallographic results on *D. vulgaris* Miyazaki cytochrome $c_{553}$ have demonstrated that the general folding pattern of the polypeptidic backbone is homologous to that of the cytochrome *c* superfamily (Nakagawa et al., 1990).

With respect to the chirality variation as a function of redox state, NMR is a unique method for affording structural insights in solution that are not available from crystal structures. In this paper, we report the sequential assignment of $^1H$ resonances of ferrocytochrome $c_{553}$ from *D. vulgaris* Hildenborough as well as the secondary structure information. The secondary structure and atypical chemical shift data have been used to reexamine the earlier sequence alignments based on amino acid sequence (Dickerson, 1980). A comparison of cytochrome $c_{553}$ 3D structural information will be discussed on the basis of the general folding pattern of the cytochromes *c*.

## EXPERIMENTAL PROCEDURES

*D. vulgaris* Hildenborough cytochrome $c_{553}$ was purified as previously reported by Le Gall and Bruschi-Heriaud (1968). Samples were reduced by addition of a 2-fold excess of disodium dithionite in phosphate buffer (0.1 M; pH = 8.0), after deoxygenating the protein solution with argon gas. Three different samples, prepared in phosphate buffer (0.1 M; pH = 5.9), were used for the NMR study: two samples in 90% $H_2O$/10% $D_2O$ and one in $D_2O$. The $D_2O$ sample was obtained after successive lyophilization and incubation for 1 h at 35 °C. The protein concentration was 5.2 mM, except for three-dimensional NMR experiments where the protein concentration was 8.0 mM. It was observed that long-term storage over several months did not lead to subtle changes in the samples, as monitored by two-dimensional NMR.

All NMR data were recorded on a Bruker AM-600 X operating at $^1H$ = 600 MHz. Spectra shown in this paper were obtained at 37 °C, but some resolution ambiguities were resolved using data acquired at 23 °C. Chemical shifts were calibrated with respect to $H_2O$, calibrated in turn at 4.658 ppm at 37 °C with 2,2-dimethyl-2-silapentane-5-sulfonate (DSS). Two-dimensional (2D) spectra were processed using either the UXNMR software of the Bruker spectrometer or Felix software provided by Hare Research, Inc. (Bothell, WA). All 2D spectra were recorded in the phase-sensitive mode using the hypercomplex method (States et al., 1982). *J*-correlated spectra were obtained by either double-quantum-filtered COSY[1] (Rance et al., 1983) or HOHAHA (Davis & Bax, 1985) experiments and NOE-correlated spectra by NOESY (Macura et al., 1981) experiments. For NOESY and HOHAHA spectra in $H_2O$ buffer, the water resonance was eliminated by a combination of weak presaturation ($\gamma B_2 \approx 50$ Hz) (with the irradiation both frequency and phase locked to the observation pulses) and jump-and-return (Plateau & Guéron, 1982) just prior to the detection period. This combination yields to a flatter base line and eliminates any danger of radiation damping and thus of receiver overflow. To reduce the frequency-dependent phase correction, the first pulse $90°_x$ was replaced by the composite pulse proposed by Freeman et al. (1988) ($[90°_x]^{-1} = 360°_x - 270°_{-x}$). Additional information was obtained from a homonuclear HOHAHA–NOESY three-dimensional experiment (HOHAHA mixing = 65 ms, NOESY mixing = 150 ms) (Simorre & Marion, 1991). In all isotropic mixing experiments (2D or 3D), the WALTZ-17 mixing scheme was optimized for balancing longitudinal and rotating-frame cross-relaxation according to the technique known as "clean TOCSY" (Griesinger et al., 1988).

## RESULTS

(*1*) *Sequential Resonance Assignment.* $c_{553}$ contains 79 amino acids, which are divided among 33 unique (11 glycines, 13 alanines, 5 leucines, 1 isoleucine, 2 valines, and 1 threonine), 21 AMX (6 tyrosines, 1 histidine, 5 aspartic acids, 1 asparagine, 6 serines, 2 cysteines, no phenylalanine, and no tryptophan), and 25 long (12 lysines, 1 proline, 5 methionines, 1 arginine, 5 glutamines, and 1 glutamic acid) spin systems.

Valuable information was obtained from spectra recorded in $D_2O$ where the small number of NH remaining greatly simplifies the data. In this respect, the assignments of helical fragments are more straightforward (all NH except the first four in the helix are actually hydrogen bonded and thus not readily exchanged in $D_2O$) than that of $\beta$-sheets where only every second residue of the peripheral strand is solvent protected. In the $D_2O$ spectra of cytochrome $c_{553}$ at pH = 5.9, 14 NH are not solvent exchanged after several days and most of these are not exchanged for several months. In view of the NH to NH crosspeaks in NOESY spectra, the slowly exchanging NH can be ascribed to two helical fragments, 38→42 and 69→77. As data recorded in $D_2O$ exhibit better signal-to-noise ratio and less base-line distortion than those in $H_2O$, these two fragments were primarily assigned using $D_2O$ spectra.

The assignment of some spin systems is documented in Figure 1. Except for a few residues (see below), the resonances exhibit reasonably narrow line width, and consequently, the spin systems can generally be delineated from the NH up to the very end of the side chain in a 50-ms HOHAHA spectrum. Such an example is provided by the $\epsilon CH_2$ of Lys 62 and Lys 70, which are connected via isotropic mixing to their respective NH (Figure 1).

Starting points for the assignment were simple residues with characteristic HOHAHA patterns such as Ala or Gly. Two alanines exhibit rather peculiar chemical shifts: Ala 4, whose $C^\alpha H$ is shifted upfield to 2.55 ppm, and Ala 22, whose $CH_3$ is at −0.88 ppm. This second signal, clearly outside the regular chemical range, has been previously identified as an alanine by Senn and co-workers (Senn et al., 1983) in their 1D NOE studies of $c_{553}$. The cause of these large perturbations in chemical shifts, likely related to the ring current of the heme, cannot be accounted for before the 3D structure of this protein is obtained. Except for Gly 18, the two $C^\alpha H$ protons of the glycines are not degenerate and show well-resolved $C^\alpha H$ to $C^\alpha H$ crosspeaks in the DQF-COSY spectrum recorded in $D_2O$ (data not shown) with large coupling constants indicative of geminal protons. Two NH to $C^\alpha H$ crosspeaks

[1] Abbreviations: COSY, *J*-correlated spectroscopy; HOHAHA, homonuclear Hartman–Hahn (correlation) spectroscopy; NOESY, nuclear Overhauser effect (correlation) spectroscopy; $c_{553}$, *Desulfovibrio vulgaris* Hildenborough cytochrome $c_{553}$; $c_{551}$, *Pseudomonas aeruginosa* cytochrome $c_{551}$.

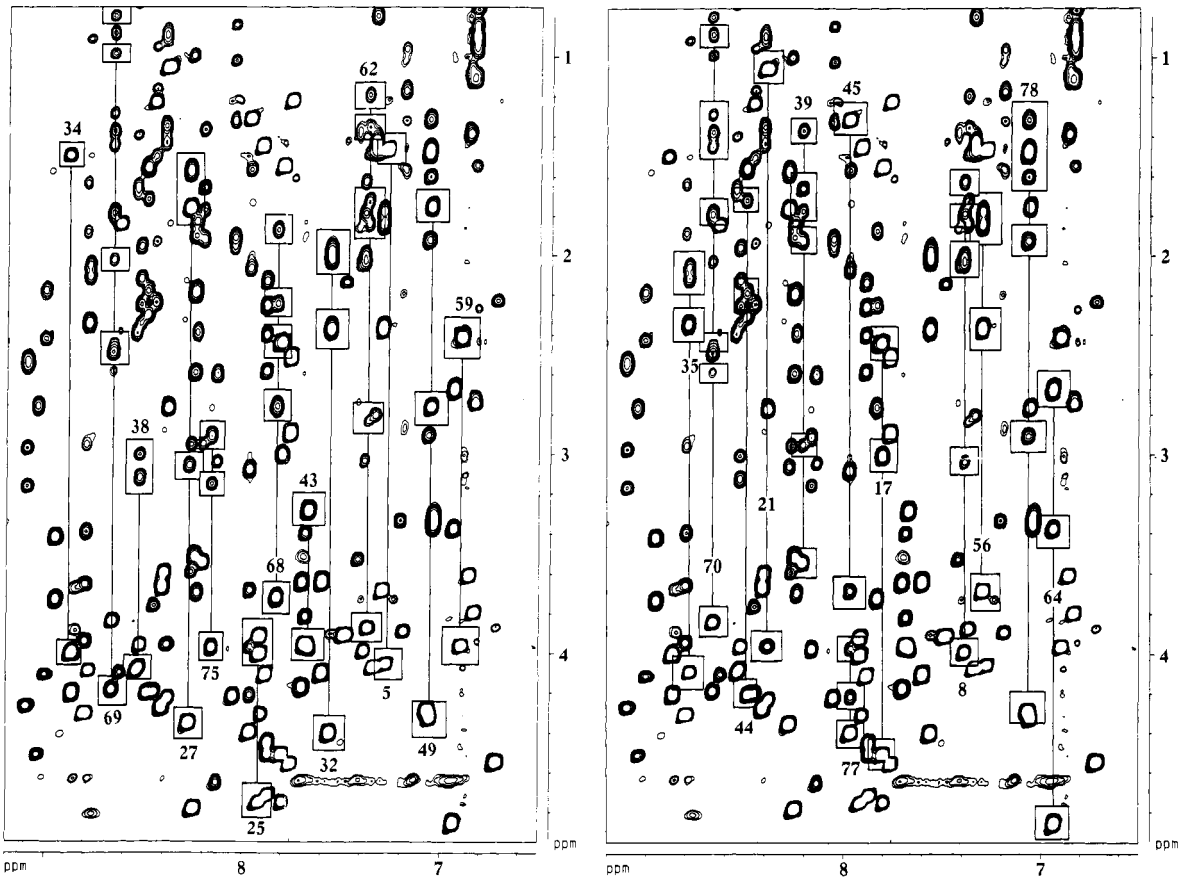


FIGURE 1: 50-ms HOHAHA spectrum of cytochrome $c_{553}$ recorded at 37 °C in $H_2O$. Care hase been taken in order to balance the rotating-frame and longitudinal Overhauser effect ("clean TOCSY"). For sake of clarity, only 25 residues have been labeled, although most of the NH show connectivities to almost all side-chain protons, even for long chains (see Lys 78, for example). The few exceptions are the N-terminal amino acids, which experience large mobility, and Gly 12 and Ala 16, which are close to the heme (see text). The left and right panels display the same spectrum but with different labels.

are detected in the DQF-COSY spectrum recorded in $H_2O$ (see Figure 2) for all Gly except for Gly 50 and Gly 51, where one of NH → $C^{\alpha}H$ crosspeaks disappears because of the small $^3J$-coupling value. However, in the HOHAHA spectrum, where the magnetizations can alternatively be transferred via the geminal coupling, one observes a pair of NH to $C^{\alpha}H$ peaks for each glycine.

Cytochrome $c_{553}$ contains only one threonine residue (at position 58), which was easily assigned. It should be noted that the $C^{\beta}H$ is downfield shifted with respect to the $C^{\alpha}H$. Although the similar intensity of the HOHAHA crosspeaks ($C^{\alpha}H$ to NH and $C^{\beta}H$ to NH) may be misleading, a clear discrimination is provided in the DQF-COSY spectrum.

The six tyrosines of cytochrome $c_{553}$ have been assigned as AMX spin systems with NOE crosspeaks to ring protons. The spectral appearance of the ring protons (in NOESY and HOHAHA spectra) depends upon the ring flip rate compared to the chemical shift differences. For nonhindered tyrosines, the $H_2$ and $H_6$ protons (as well as the $H_3$ and $H_5$ protons) are in symmetry-related equivalent positions, leading to a single narrow signal for each pair (Wagner et al., 1976; Wüthrich, 1986); this case is found for Tyr 38, 49, and 64 (see Figure 3). For intermediate flipping rates resulting from steric hinderance, a significant line broadening arises due to chemical exchange as shown for the three remaining tyrosines (7, 44, and 75). The line broadening is a function of both the flip rate and the chemical shift of the protons in each of the blocked states. As a result, the broader signal can be either that of the $H_2$,$H_6$ pair or that of the $H_3$,$H_5$ pair. The discrimination between these two pairs for each Tyr cannot be based on chemical shift but only on distance estimates to the $C^{\beta}H_2$ corrected for spin diffusion. However, precise integration of broad signals is never accurate, and the assignments given in Table I for the ring protons of Tyr 7, 44, and 75 should be considered the most likely. Note that the line broadening due to ring flip, which is temperature dependent, provides insight into the dynamical behavior of this cytochrome, and a quantitative interpretation will be published elsewhere. Finally, we point out that, over a wide range of temperature (20 to 45 °C), the $H_{2,6}$ and the $H_{3,5}$ signals of Tyr 38 overlap, and the NH resonance of Tyr 64 is almost at the same frequency as its $H_{3,5}$ signal.

The overlap of the NH of Cys 13 with the NH of His 14 has not been resolved by acquiring spectra at different temperatures. In the HOHAHA spectrum, two AMX spin systems were identified: one at 4.33, 1.45, and 0.75 ppm and another at 2.98, 1.76, and 1.08 ppm. Histidine $C^{\beta}H_2$ protons are usually assigned on the basis of NOESY crosspeaks with their ring protons, but in the present case, this crosspeak is expected in a very crowded spectral region due to the unusual chemical shifts (0.93 and 0.34 ppm) of His 14 ring protons (Senn et al., 1983). Definite assignment of His 14 and Cys 13 is supported by detection of NOESY peaks between the $C^{\beta}H_2$ of Cys 13, on the one hand, and both the methine 4 and meso $\beta$ protons of the heme, on the other hand.

Due to the high signal-to-noise ratio of our data, most of the NH(i) → NH($i$+1) NOE connectivities were detected simultaneously with those of the $C^{\alpha}H(i)$ → NH($i$+1), although their intensities strongly vary as functions of secondary structure. The only exceptions are located at the N-terminus

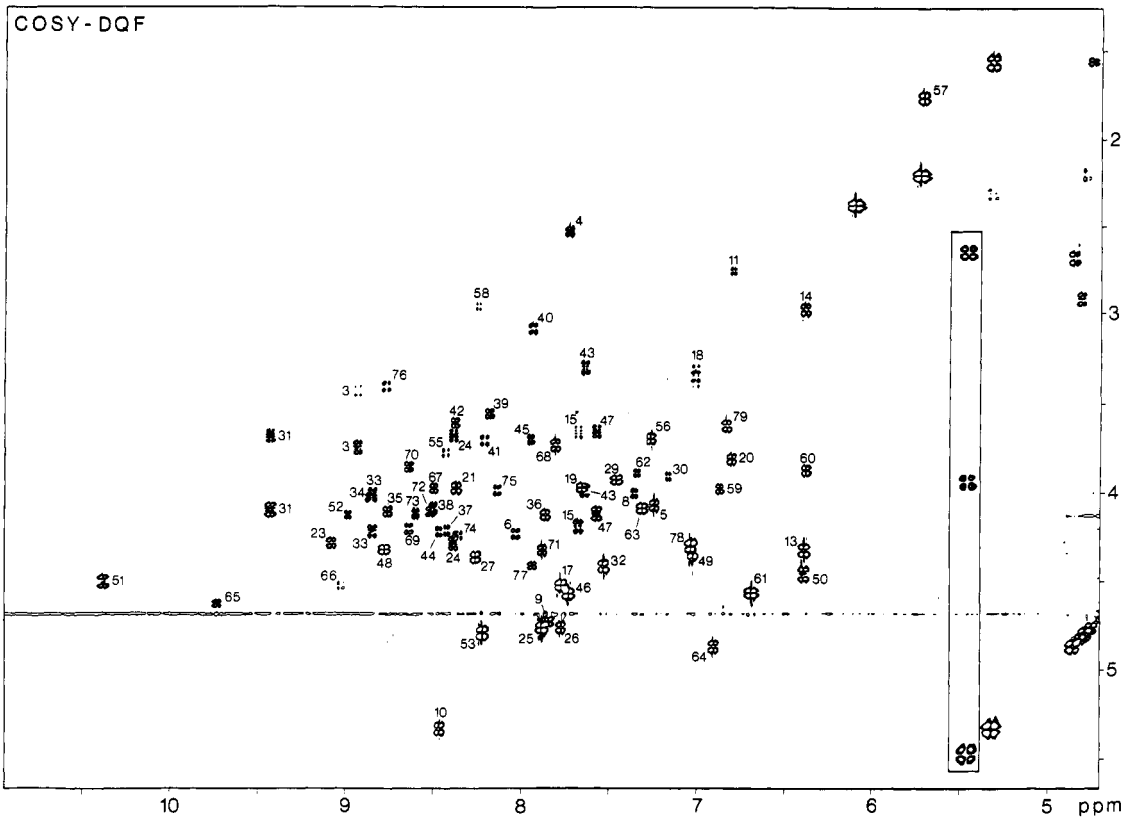


FIGURE 2: Double-quantum-filtered COSY spectrum of cytochrome $c_{553}$ at 37 °C in $H_2O$. The horizontal noise line corresponds to the residual water signal, for which suppression has been optimized to minimize the number of missing crosspeaks. The most downfield shift NH is assigned to Gly 51, and this unusual shift, due to heme ring current shift, is also observed in other cytochromes *c* (see text and the sequence alignment in Figure 8). In the boxed area (at $F_2$ = 5.46 ppm) are indicated crosspeaks corresponding to propionate 7. This proton at 5.46 ppm exhibits two large coupling constants [a geminal ($^2J$) and a vicinal ($^3J$)], and the crosspeak to the fourth propionate proton cannot be seen, due to the associated small vicinal coupling.

and between residues 20 and 22. An illustrative example of $C^{\alpha}H(i) \rightarrow NH(i+1)$ connectivities from Lys 30 to Tyr 44 is given in Figure 4. In Figure 5, two sets of $NH(i) \rightarrow NH(i+1)$ connectivities are shown, corresponding to Ala 34 to Asp 46 and Glu 67 to Ser 77. For each pair of sequential NH–NH crosspeaks, an additional and redundant $NH(i) \rightarrow NH(i+2)$ signal of weak intensity is generally detected, in agreement with the expected short distance (4.2 Å) in helices. As noted earlier, a large part of the connectivities shown in Figure 5 have also been detected in the $D_2O$ sample and thus correspond to slowly exchanging protons.

A complete list of the proton assignment for ferrocytochrome $c_{553}$ obtained in this work at 37 °C is given in Table I. It should be noted that no stereospecific assignments (for the $C^{\beta}H_2$ of AMX spin systems and for glycines) have been included. The presence of the terminal $NH_3^+$ (as possibly some conformational flexibility) induce a line-broadening for the two N-terminal residues and prevent their complete assignment.

(*2*) *Heme Group Assignments.* Included in Table I are the assignments of the heme protons which are in close agreement with the preliminary data of Senn et al. (1983); the slight chemical shift differences can be ascribed to variation of experimental conditions (pH = 5.9 versus 7.0 and temperature of 37 °C versus 30 °C). As expected, each NOE seen in the earlier work by one-dimensional NMR coincides with a NOESY peak in our data.

From NOESY experiments, we can conclude that the covalent binding of the heme group to the polypeptidic chain is achieved through thiother bridges between Cys 10 and methine 2, and Cys 13 and methine 4, respectively.

Let us now discuss the assignment of the heme environment. In the NOESY spectrum, a group of eight protons, which split into two sets of four according to their HOHAHA network, give rise to crosspeaks to the meso $\gamma$ proton. This finding first confirms the assignment of the meso $\gamma$ proton, which is the only meso proton symmetrically located between the propionates 6 and 7. Each propionate proton is connected to three other protons in a HOHAHA spectrum, but only to two protons in a COSY-DQF spectrum (see the boxed area at 5.46 ppm in Figure 2). The geminal coupling observed is of the same order of magnitude observed for glycine, but the disappearance of the third crosspeak in COSY-DQF is due to a vanishingly small vicinal coupling, related to the propionate conformation. A quite similar pattern could been seen for the second propionate (at 4.63 ppm), but it is partially obscured by the water signal. The specific assignment for each propionate group is given by a NOESY crosspeak between the proton propionate 7 at 5.46 ppm and the methyl 8 of the heme. From the comparison with previous studies of the *P. aeruginosa* cytochrome $c_{551}$, we can conclude that the propionate chemical shifts are very sensitive to local heme environment: in both cytochromes, the axial methionine has the same *S* chirality but a different orientation [a clockwise rotation of 45° from $c_{551}$ to $c_{553}$ (Senn & Wüthrich, 1985)].

On the basis of the amino acid sequence, either Met 56 or Met 57 could be the sixth heme axial ligand. Our results clearly eliminate Met 56 as an axial ligand, in view of the unusual chemical shift of the Met 57 side chain. Moreover, Met 57 is undoubtedly identified by NOE with the following residue (the unique Thr 58) and NOESY crosspeaks to the heme group ($C^{\beta}H_2$ of Met with meso $\gamma$ and methine 2 protons).

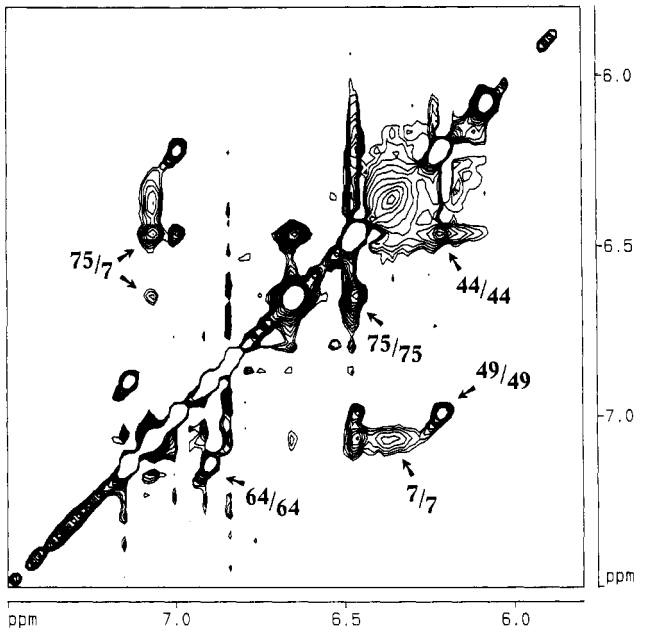


FIGURE 3: 150-ms NOESY spectrum of cytochrome $c_{553}$ at 37 °C in $D_2O$. In this expansion of the aromatic region, two groups of tyrosines can be distinguished. Nonhindered tyrosines (49 and 64) exhibit narrow signals for both degenerate $H_{2,6}$ and for the $H_{3,5}$ and thus a well-resolved intra-ring crosspeak occurs. In addition, the ring protons of Tyr 38 are fully degenerate (see Table I). On the other hand, three tyrosines (7, 44, and 75) exhibit broad signals, which provide evidence of a restricted mobility (intermediate exchange on the NMR time scale). All these intraresidue crosspeaks (labeled in the lower left corner) are also present in the HOHAHA spectrum and thus correspond to intraresidue connectivities. An additional crosspeak (upper left corner) is not detected in the HOHAHA spectrum taken in $D_2O$: it corresponds to a close distance between tyrosines 7 and 75. This contact between these residues is probably the cause of the steric hindrance which induces the reported line-broadening.

(*3*) *Secondary Structure in Cytochrome $c_{553}$.* In Figure 6 the structural information readily obtainable at this stage of the study has been summarized. Sequential NOE have been reported as well as long-range NOE which characterize helical structure (Wüthrich, 1986). For the sake of completeness, the missing pieces of information due to NMR artifacts have been indicated by stars (*) when overlaps occur and by crosses (+) when the line width of the NH prevents a reliable quantification of the NOE.

From data in Figure 6, four stretches of helices can be identified. In addition, a fifth helix is likely, but is masked by spectral artifacts (see below). The precise definition of both ends of an helical structure highly depends upon the criteria employed. Depending upon the conformational probe (sequential or long-range NOE, for instance) the length of a helix may vary by one to two residues. With these limitations in mind, the four helices are defined as follows: 2→8, 34→46, 53→59, and 67→77, for which short NH($i$)–NH($i$+1) and $C^{\alpha}H(i)$–NH($i$+3) distances are observed (Wüthrich, 1986). Since they involve a larger number of H-bonds, longer stretches of helices are likely to be more stable and to fit more closely to idealized canonic structures. For helices 34→46 and 67→77, NH($i$)–NH($i$+1) and $C^{\alpha}H(i)$–NH($i$+3) short distances define the helix limits in the same manner. On the other hand, helices 2→8 and 53→59 could be extended by several residues at the C-terminus if the criteria are relaxed. It is worth noting that an additional $C^{\alpha}H(i)$–NH($i$+2) NOE is detected at the beginning of each stretch, in agreement with a slightly distorted initiation of the helix.

Figure 5 shows the NH($i$)–NH($i$+1) crosspeaks observed for two helices of $c_{553}$. Resonance assignment in helical proteins is known to be more laborious, because of the high degree of symmetry of helices and the resulting narrow dispersion of chemical shifts. This feature is highlighted for helices 34→46 and 67→77, where the NH chemical shift remains strictly in the range 7.5–9.0 ppm for the helix core but starts to diverge at the ends (see Table I). The two other helical fragments exhibit a wider spread of chemical shifts for two reasons: they are shorter and thus probably less symmetrical, and they provide the anchor points for the heme ligands (Cys 10, Cys 13, and His 14 near helix 2→8 and Met 57 in 53→59).

Topological arguments taken from other studies of cytochromes *c* support a partial helical structure around the Cys-Xxx-Xxx-Cys-His motif so that both cysteine residues point toward the porphyrin. Unfortunately, we are not able to provide a precise description of this segment because the NH of Gly 12 and Ala 16 exhibit an atypical line broadening (the latter residue cannot be detected at 37 °C, and its position has been inferred from low-temperature experiments; data not shown). The close distance between the heme and residues 12 and 14 is in agreement with their line broadening. Nonetheless, the four residue distance between Gly 12 and Ala 16 support a secondary structure which could be seen either as a short pseudohelical fragment or as a turn. Line-broadening of resonances in metalloproteins is a frequent feature. Several mechanisms can account for it, such as residual paramagnetism (for instance, in Fe-S proteins) (Oh & Markley, 1990) or a conformational exchange process related to the high anisotropy of the heme group (Schulman et al., 1970). Residual paramagnetism can be ruled out in the case of a fully reduced cytochrome. The latter interpretation is on the other hand supported by a recent study of mutants of reduced Iso-1-cytochrome *c* from *Saccharomyces cerevisiae*: Gao et al. (1991) have observed that a mutation at position 82 (i.e., on the opposite side of the heme) induces chemical shift variations larger than 0.1 ppm for some residues close to the covalent heme linkage.

(*4*) *Intramolecular Interaction of Segments of the Core.* In the NOESY spectrum of the aromatic region displayed in Figure 3, some crosspeaks cannot be interpreted as intraresidue NOE contacts, even if the chemical exchange at intermediate rates is taken into account. The $H_{2,6}$ protons of the Tyr 7 ring show connectivities to the ring protons of Tyr 75, indicating that the portions of the N-terminal (2→8) and the C-terminal (67→77) helices are in close proximity. This finding is corroborated by an additional short distance between the ring protons of Tyr 7 and the $C^{\delta}H_3$ of Leu 72 observed in a homonuclear HOHAHA–NOESY experiment (spectrum not shown).

Figure 7 shows another piece of information provided by 3D NMR: on the left-hand side, a slice has been taken at the chemical shift of one of the $C^{\beta}H_2$ of Lys 70 and the HOHAHA pattern corresponding to this residue is NOE transferred to both NH of Lys 70 and Ala 71. The right-hand panel (taken at the chemical shift of $C^{\alpha}H$ of Lys 70) shows the transfer of the Lys 70 pattern to the ring protons of Tyr 38. Assignment of long-range NOE such as these is crucial because mistakes can lead to completely erroneous 3D structure. In this respect, it should be pointed out that NOE are assigned on the sole basis of chemical shift in 2D NMR but that, in 3D NMR, the HOHAHA pattern associated with a NOESY peak is the indelible signature of one of the NOE partners (Simorre & Marion, 1991). In summary, a close

Table I: Chemical Shifts of $c_{553}$ at 37 °C

| | NH | $C^{\alpha}H$ | $C^{\beta}H$ | others | | NH | $C^{\alpha}H$ | $C^{\beta}H$ | others |
|---|---|---|---|---|---|---|---|---|---|
| Ala 1 | | | | | Met 41 | 8.23 | 3.70 | 1.82, 1.78 | 2.40 |
| Asp 2 | 7.75 | 4.83 | | | Lys 42 | 8.39 | 3.61 | 1.36, 1.45 | 0.92, 0.92 |
| Gly 3 | 8.94 | 3.44, 3.75 | | | Gly 43 | 7.65 | 3.98, 3.30 | | |
| Ala 4 | 7.75 | 2.55 | 1.24 | | Tyr 44 | 8.48 | 4.22 | 2.20, 1.73 | $H_{2,6} \simeq 6.25$; $H_{3,5}$ 6.50 |
| Ala 5 | 7.26 | 4.08 | 1.48 | | Ala 45 | 7.97 | 3.70 | 1.33 | |
| Leu 6 | 8.03 | 4.24 | 1.93, 1.34 | 1.98; $\delta CH_3$ 0.86, 1.04 | Asp 46 | 7.74 | 4.58 | 2.90, 2.53 | |
| Tyr 7 | 8.12 | 4.68 | 2.61, 3.05 | $H_{2,6}$ 7.11; $H_{3,5} \simeq 6.40$ | Gly 47 | 7.59 | 3.66, 4.12 | | |
| Lys 8 | 7.38 | 4.01 | 2.03, 2.05 | 1.64, 1.80; $\epsilon CH_2$ 3.04 | Ser 48 | 8.78 | 4.33 | 3.98, 3.67 | |
| Ser 9 | 7.86 | 4.73 | 4.47, 4.52 | | Tyr 49 | 7.03 | 4.33 | 2.78, 1.77 | $H_{2,6}$ 6.27; $H_{3,5}$ 7.03 |
| Cys 10 | 8.48 | 5.33 | 1.57, 2.32 | | Gly 50 | 6.41 | 3.04, 4.47 | | |
| Ile 11 | 6.82 | 2.78 | 1.56 | $CH_3$ 0.78, 1.00 | Gly 51 | 10.39 | 4.52, 3.92 | | |
| Gly 12 | 8.83 | 3.69, 3.91 | | | Glu 52 | 8.99 | 4.13 | 2.19, 2.21 | 2.44 |
| Cys 13 | 6.41 | 4.33 | 1.45, 0.75 | | Arg 53 | 8.23 | 4.79 | 2.18, 2.20 | 1.88, 1.83 |
| His 14 | 6.41 | 2.98 | 1.76, 1.08 | ring 0.93, 0.34 | Lys 54 | 7.41 | 3.54 | 2.06, 1.40 | 1.84; $\epsilon CH_2$ 2.72 |
| Gly 15 | 7.69 | 3.66, 4.19 | | | Ala 55 | 8.44 | 3.78 | 1.25 | |
| Ala 16[a] | | | 1.45 | | Met 56 | 7.28 | 3.70 | 1.79, 1.87 | 2.38, 2.38 |
| Asp 17 | 7.79 | 4.53 | 2.45, 3.02 | | Met 57 | 5.73 | 1.77 | −0.65, −1.76 | −3.56, −3.79; $\epsilon CH_3$ −3.56 |
| Gly 18 | 7.03 | 3.33, 3.36 | | | Thr 58 | 8.24 | 2.97 | 3.61 | 1.01 |
| Ser 19 | 7.68 | 3.97 | 3.83, 3.42 | | Asn 59 | 6.88 | 3.98 | 2.43, 2.43 | $NH_2$ 7.38, 6.77 |
| Lys 20 | 6.82 | 3.81 | 0.88, 0.92 | $\delta CH_2$ 1.10; $\epsilon CH_2$ 2.72 | Ala 60 | 6.40 | 3.88 | 0.25 | |
| Ala 21 | 8.38 | 3.97 | 1.07 | | Val 61 | 6.70 | 4.56 | 2.24 | 0.34, 0.02 |
| Ala 22 | 7.18 | 3.35 | −0.88 | | Lys 62 | 7.35 | 3.89 | 1.75, 1.86 | 1.21, 1.37 |
| Met 23 | 9.08 | 4.28 | 2.54, 2.60 | 2.99, 3.18 | Lys 63 | 7.32 | 4.09 | 1.43, 1.48 | 0.63, 0.83; $\epsilon CH_2$ 2.78 |
| Gly 24 | 8.40 | 3.68, 4.29 | | | Tyr 64 | 6.92 | 4.87 | 2.69, 3.39 | $H_{2,6}$ 7.18; $H_{3,5}$ 6.93 |
| Ser 25 | 7.92 | 4.77 | 4.02, 3.94 | | Ser 65 | 9.72 | 4.63 | 4.47, 4.11 | |
| Ala 26 | 7.78 | 4.77 | 1.56 | | Asp 66 | 9.03 | 4.53 | 2.76, 2.79 | |
| Lys 27 | 8.25 | 4.37 | 1.57, 1.78 | −; $\epsilon CH_2$ 3.06 | Glu 67 | 8.51 | 3.98 | 2.14, 1.97 | 2.37, 2.26 |
| Pro 28 | | 3.87 | 1.98, 1.68 | | Glu 68 | 7.82 | 3.74 | 2.27, 1.89 | 2.78, 2.46 |
| Val 29 | 7.47 | 3.93 | 2.15 | 0.34, −0.10 | Leu 69 | 8.65 | 4.20 | 2.48, 2.51 | 2.05; $\delta CH_3$ 1.01, 0.81 |
| Lys 30 | 7.18 | 3.90 | 1.20, 1.60 | 1.00, 0.86; $\epsilon CH_2$ 2.87 | Lys 70 | 8.66 | 3.85 | 1.80, 0.85 | 1.35; $\delta CH_2$ 1.34, 1.25; $\epsilon CH_2$ 2.41, 2.55 |
| Gly 31 | 9.41 | 3.68, 4.10 | | | | | | | |
| Gln 32 | 7.54 | 4.42 | 1.98, 2.02 | 2.38; $NH_2$ 7.39, 8.59 | Ala 71 | 7.90 | 4.33 | 1.47 | |
| Gly 33 | 8.83 | 4.02, 4.22 | | | Leu 72 | 8.52 | 4.11 | 2.40, 2.40 | 1.70; $\delta CH_3$ 1.41, 0.75 |
| Ala 34 | 8.87 | 4.02 | 1.51 | | Ala 73 | 8.62 | 4.13 | 1.86 | |
| Glu 35 | 8.78 | 4.11 | 2.06, 2.13 | 2.35, 2.35 | Asp 74 | 8.37 | 4.25 | 2.79, 2.79 | |
| Glu 36 | 7.87 | 4.12 | 2.15, 2.28 | 2.41, 2.61 | Tyr 75 | 8.15 | 3.99 | 3.17, 2.93 | $H_{2,6} \simeq 6.69$; $H_{3,5}$ 6.51 |
| Leu 37 | 8.44 | 4.22 | 2.26 | 1.95; $\delta CH_3$ 1.18, 0.97 | Met 76 | 8.78 | 3.41 | 2.37 | 1.90, 1.65; $\epsilon CH_3$ 2.98 |
| Tyr 38 | 8.52 | 4.09 | 3.02, 3.13 | $H_{2,6}$ and $H_{3,5}$ 6.87 | Ser 77 | 7.95 | 4.42 | 4.23, 3.99 | |
| Lys 39 | 8.19 | 3.56 | 1.94, 1.78 | 1.67, 1.39; $\epsilon CH_2$ 2.95 | Lys 78 | 7.05 | 4.31 | 2.92, 1.93 | 1.59, 1.50, 1.48, 1.33 |
| Lys 40 | 7.95 | 3.09 | 2.09, 1.59 | 0.35, 1.77, 2.25 | Leu 79 | 6.84 | 3.62 | 1.40, 1.07 | 1.13; $\delta CH_3$ 0.34, 0.09 |

| heme | | | | | | | | | |
|---|---|---|---|---|---|---|---|---|---|
| meso H | | ring Me | | *S*-methyne | | methyl | | 7-propionate | 6-propionate |
| $\alpha$ | 9.62 | 1 | 3.95 | 2 | 5.75 | 2 | 2.20 | 5.46 | 4.63 |
| $\beta$ | 9.19 | 3 | 3.75 | 4 | 6.13 | 4 | 2.39 | 3.95 | 2.29 |
| $\gamma$ | 10.07 | 5 | 3.36 | | | | | 3.44 | 2.04 |
| $\delta$ | 9.29 | 8 | 3.39 | | | | | 2.65 | 1.56 |

[a] Ala 16 cannot be seen at 37 °C. NH = 9.47 ppm, $C^{\alpha}H$ 4.88 ppm, and $C^{\beta}H_3$ = 1.42 ppm at 23 °C.

distance between the $C^{\alpha}H$ of Lys 70 and the ring of Tyr 38 is definitively identified, and consequently between the 34→47 helix and the C-terminal helix (67→77).

Further interpretation of long-range NOESY data is still in progress in our laboratory in order to provide the basis for calculation of the cytochrome $c_{553}$ structure. However, these qualitative data demonstrate that helices 2→8 and 34→46 are spatially near the C-terminal helix 67→77, in agreement with the general folding pattern of cytochrome *c*, a point which will be discussed in detail in the following section.

## DISCUSSION

*(1) Comparison with the Crystal Structure of D. vulgaris Ferricytochrome* $c_{553}$. We have obtained an almost complete set of assignments for ferrocytochrome $c_{553}$ from *D. vulgaris* Hildenborough. On the basis of the observation of long stretches of $d_{NN}(i,i+1)$ and $d_{\alpha N}(i,i+3)$ connectivities (see Figure 6), strong evidence for four helical regions could be found. These data agree with the X-ray structure of ferricytochrome $c_{553}$ from *D. vulgaris* Miyazaki (Nakagawa et al., 1990). It should be remembered that these two proteins share 63 identical residues (of 79), while 15 positions show conservative amino acid replacements (van Rooijen et al., 1989). The two lower lines of Figure 8 display the sequence alignment for the two cytochromes $c_{553}$ with experimentally detected helices depicted in bold font. Within an accuracy of one residue, the four helices align (helices 2→8, 34→46, 53→59, and 67→77). Although spectral parameters of residues 12 and 16 are not available due to line-broadening (discussed above), a fifth helix cannot be ruled out at position 11–14. Further comparison of our data with those of Nakagawa et al. (1990) is not possible as only the $\alpha$-carbon structure is reported in this paper and data on side-chain conformations are not yet available. Let us finally note that Met 56 of *D. vulgaris* Hildenborough is replaced by a valine in *D. vulgaris* Miyazaki, a fact which clearly rules out Met 56 as sixth heme ligand in our case.

*(2) Structural Comparison with Other Cytochromes c.* Crystallographic and NMR studies on miscellaneous cytochromes *c* have led to the proposal of a common folding

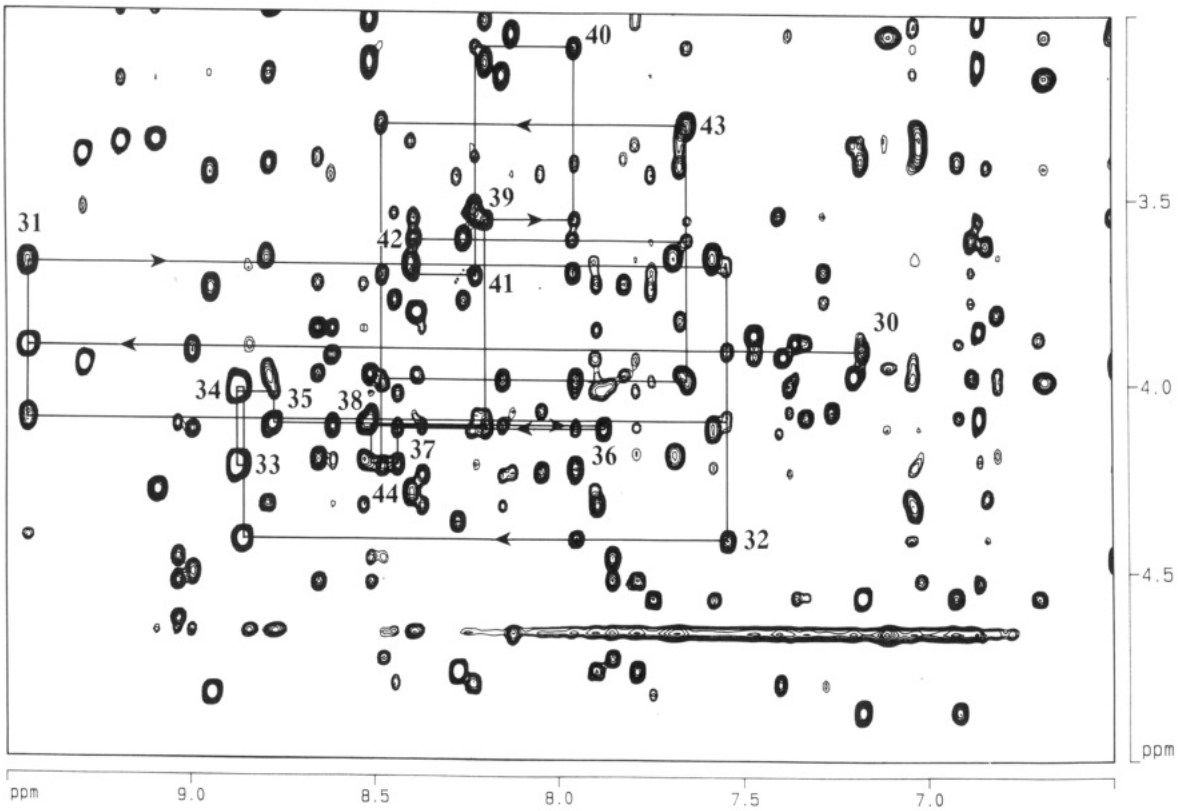


FIGURE 4: 150-ms NOESY spectrum of cytochrome $c_{553}$ at 37 °C in $H_2O$. The sequential C$\alpha$H($i$) → NH($i$+1) connectivities for residues 30–44 are shown, and the assignment is confirmed by NH($i$) → NH($i$+1) connectivities (see Figure 5). The partial overlap of the C$^{\alpha}$H and NH of Gly 33 and Ala 34 has made their assignment difficult, but could be resolved by changing the temperature to 23 °C.

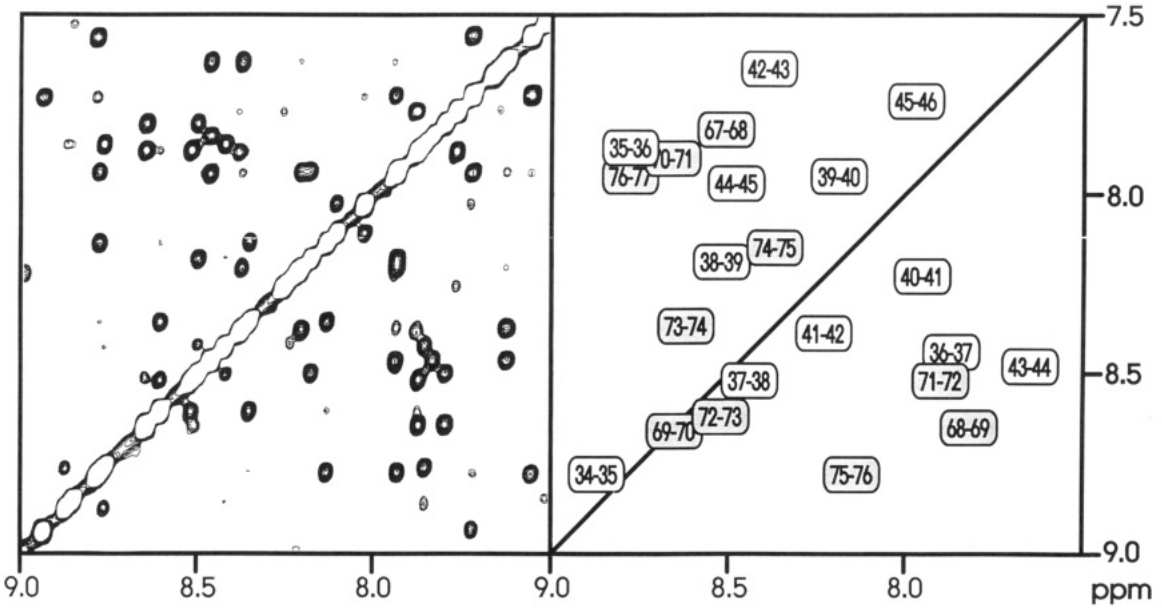


FIGURE 5: 150-ms NOESY spectrum of cytochrome $c_{553}$ at 37 °C in $H_2O$. The NH($i$) → NH($i$+1) connectivities are shown for two fragments of helices [from Ala 34 to Asp 46 and from Glu 67 to Ser 77 (shaded labels)]. These residues correspond to the most stable region of the cytochrome (helices C and D in Figure 9), as shown by the slow exchange rate for most of them (see text and Figure 6). The labels is the right-hand panel can be superimposed on the spectrum of the left-hand panel. The very symmetrical nature of the helix does not introduce much of chemical shift dispersion for the NH of these residues, which are found without exception between 7.5 and 9.0 ppm.

pattern for this protein family (Chothia & Lesk, 1985). As a matter of fact, three $\alpha$-helices are highly conserved as depicted in Figure 8, specifically, the 3→12 N-terminal helix and the 61→75 (with a break at Pro 71) and the 88→101 C-terminal helix (numbering according to horse cytochrome). Close contacts between the two first helices and the C-terminal helix are supported by our long-range NOE data reported above (Tyr 7 → Tyr 75, Tyr 7 → Leu 72 and Tyr 38 → Lys 70). Similar long-range NOE have been described in a NMR study of horse ferricytochrome *c* (Feng et al., 1989) [Phe 10 → Tyr 97 (horse numbering)] and in the study of ferrocytochrome $c_{551}$ of *P. aeruginosa* (Detlefsen et al., 1990) (Phe 7 → Trp 77).

Figure 9 depicts a crude model of both cytochromes $c_{551}$ and $c_{553}$, which illustrates the relative location of the helices with respect to the heme. This schematic drawing is not intented to provide a precise description of the structure of these cytochromes (that of cytochrome $c_{553}$ is presently being

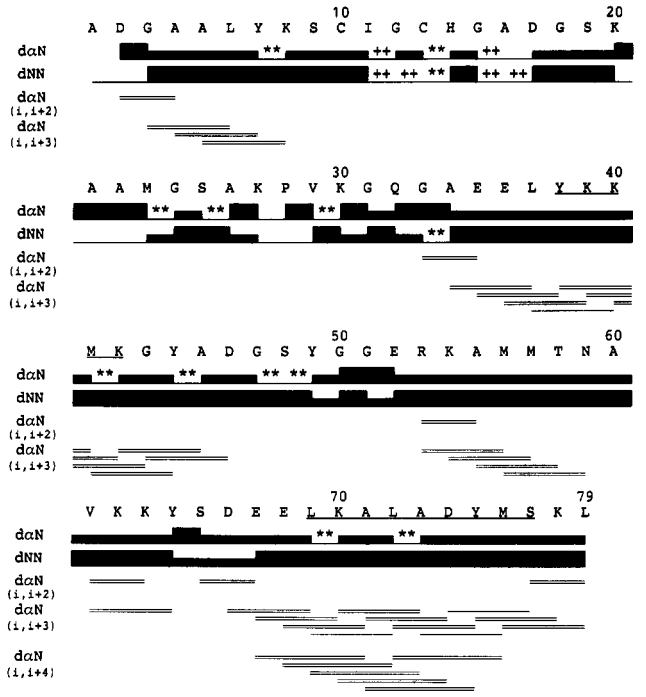


FIGURE 6: Sequence of the cytochrome $c_{553}$ from *D. vulgaris* Hildenborough with a schematic summary of the sequential connectivities which supports the resonance assignment. Missing connectivities due to spectral artifacts are discriminated from those which have a conformational relevance. Stars (*) indicate peaks which cannot be seen because of spectral overlap and crosses (+) peaks which are line broadened (see text). Underlined residues (38–41 and 69–77) correspond to slowly exchanging protons (lifetime greater than a few weeks at room temperature and pH = 5.9). For long-range NOE, $d_{\alpha N}(i,i+2)$, $d_{\alpha N}(i,i+3)$, and $d_{\alpha N}(i,i+4)$, a double line indicates clearly evidenced connectivities, while a single line corresponds to cases where spectral overlap prevents a definite assignment of these crosspeaks. $d_{\alpha N}(i,i+4)$ have only been detected for the C-terminal helix.

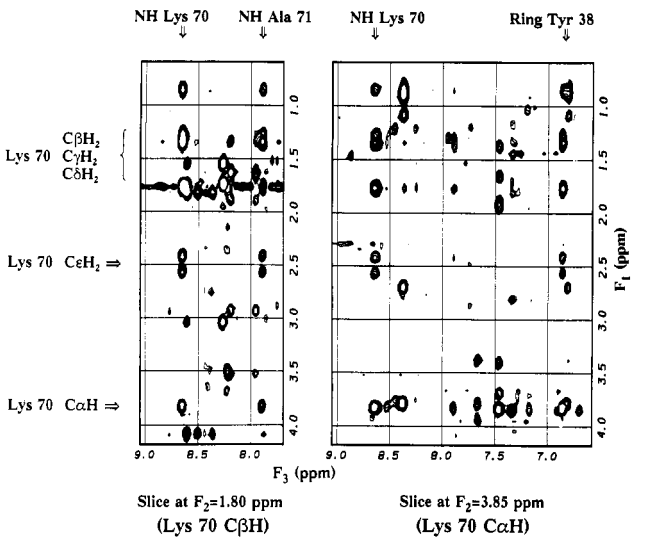


FIGURE 7: 2D slices of the 3D HOHAHA-NOESY spectrum of cytochrome $c_{553}$. This figure illustrates the assignment of a long-range NOE between the $C^{\alpha}H$ of Lys 70 and the degenerate protons of the Tyr 38 ring. As a large number of $C^{\alpha}H$ are observed in region surrounding 3.85 ppm, additional arguments for the assignment of Lys 70 are required. On the left-hand panel, the HOHAHA pattern of Lys 70 is first identified. In this slice taken at $F_2$ = 1.80 ppm (i.e., one of the $C^{\beta}H_2$ of Lys 70), the pattern for Lys 70 is transferred via NOE to both the NH of 70 and that of 71. Moving to the slice at $F_2$ = 3.85 ppm (i.e., the $C^{\alpha}H$ of Lys 70), one observes that the Lys 70 HOHAHA pattern is NOE transferred to a single narrow signal corresponding to the Tyr 38 ring. This figure provides unequivocal assignment for only one NOE partner ($C^{\alpha}H$ of Lys 70) and the identification of Tyr 38 ring protons should be backed up by a similar reasoning. Unfortunately, the chemical shift degeneracy of the ring protons of Tyr 38 prevents the observation of any HOHAHA pattern.

```
Horse c      G D V E K G K K I F V Q K - C A Q C H T V E K G G K H K T G P N L H G L F G R K
                    10                  20                  30
P.a. c551      E D P E V L F K N K G C V A C H A I D - T - K M V G - P A Y K D V A A K -
               1                  10                  20                  30
D.v.M. c553    A D G A A L Y K S - - C V G C H G A D - G S K - Q A M G V G H A V - - K -
               1                  10                  20                  30
D.v.H. c553    A D G A A L Y K S - - C I G C H G A D - G S K - A A M G S A K P V - - K -
               1                  10                  20                  30

Horse c      T G Q A P G F T Y T D A N K N K G I T W K E E T L M E Y L E N P K K Y I - - - -
             40                  50                  60                  70
P.a. c551      - - - - - - - - - - - - - - - - - - F A G Q A G A E A E L A Q R I K N G S Q G - -
                                                   40                  50
D.v.M. c553    - - - - - - - - - - - - - - - - - - - - G Q K - A D - E L F K K L K G Y A D G S Y
                                                       40
D.v.H. c553    - - - - - - - - - - - - - - - - - - - - G Q G - A E - E L Y K K M K G Y A D G S Y
                                                       40

Horse c      - - - P G T K M I F A G I K - K - K T E R E D L I A Y L K K A T N E
                    80                  90                  100
P.a. c551      - V W G P I P M P P N A V - - - S D D E A Q T L A K W V L S Q K
                    60                  70                  80
D.v.M. c553    G G E K K A V M T N - L V K R Y S D E E M K A M A D Y M S K L
               50                  60                  70
D.v.H. c553    G G E R K A M M T N - A V K K Y S D E E L K A L A D Y M S K L
               50                  60                  70
```

FIGURE 8: Structural sequence alignment of four *c*-type cytochromes on the basis of an NMR study of horse cytochrome *c* (Feng et al. 1989), an NMR study of *P. aeruginosa* cytochrome $c_{551}$ (Detlefsen et al., 1990), preliminary X-ray data on cytochrome $c_{553}$ from *D. vulgaris* Miyazaki (Nakagawa et al., 1990), and present NMR data on cytochrome $c_{553}$ from *D. vulgaris* Hildenborough. Residues indicated in large bold font are involved in helical structures according to the authors mentioned above. The sequence alignment is adapted from that of Dickerson (1980) with slight modifications directed at aligning the secondary structure elements and the observed atypical chemical shifts (see text). For each protein, the relevant residue numbering is given for sake of clarity.

determined) but highlights the location of the various helices within the general fold of small MW cytochrome *c*. Helices labeled D and F in Figure 9, which are highly conserved in all cytochromes *c*, have been demonstrated to form the back of the heme pocket (Takano & Dickerson, 1981). Besides these common features, an additional (but different) helix is also present in each cytochrome shown in Figure 8. For example, in the eukaryotic cytochromes, a short helix (50→55) occurs close to heme pocket on its propionic acid side, which corresponds to a deleted segment (39→57) in the case of $c_{551}$ and $c_{553}$. The schematic drawing of Figure 9 shows that the major difference between the two bacterial proteins occurs in helical segments 27→33 of cytochrome $c_{551}$ (helix C) and 54→59 of cytochrome $c_{553}$ (helix E). We note that these structural differences could have a significant role in redox properties of these proteins. It is important to keep in mind that the major difference between these two proteins lies in their respective redox potential (10 mV for $c_{553}$ versus +260mV for $c_{551}$).

As mentioned above, the delineation of helical structures is subject to diverse assessment from different authors. Although the 14→20 fragment in horse cytochrome as well as the corresponding of $c_{551}$ have not been pictured as helices in the X-ray structure, NMR data for $c_{551}$ (Detlefsen et al., 1990) and $c_{553}$ (this study) are compatible with a helix.

From our results and previously published data, distinctions between the functional importance of the various helices can be made. The three conserved helices are intrinsic structural features of this protein family as opposed to the nonconserved helices. This latter group can be interpreted as a method used by nature to both connect the conserved helices and partially bury the hydrophobic heme group. When the number of residues involved in these junction elements is sufficient, a stabilized helix is built. Alternatively, a less stable but more direct connection occurs for which no regular structure is assembled. This trend can be illustrated in two ways: the 27→33 helix (helix C) in $c_{551}$ corresponds to few deletions in

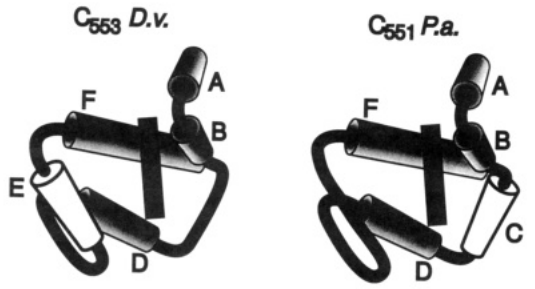


FIGURE 9: Location of the helical fragments of *D. vulgaris* Hildenborough cytochrome $c_{553}$ and *P. aeruginosa* cytochrome $c_{551}$. Because the tertiary structure of *D. vulgaris* H. is not yet known, this schematic drawing only indicates location in the sequence but not in space. Within the general folding of the cytochrome *c*, four helices (labeled A, B, D, and F) are conserved, whereas one additional helix is found in each protein (helix C in cytochrome $c_{551}$ and helix E in $c_{553}$). When the length of the connection element is suitable, a helix occurs instead of a less structured element.

$c_{553}$ (see sequence alignment in Figure 8), and the observed helix in the present case around the Met 57 heme ligand (helix E) is not feasible in $c_{551}$ because of the unusually large number of prolines in this region (Pro 58 to Pro 63).

In a similar manner, comparison between nonstructured parts of the protein can be drawn. Segments 14→20, 27→33, and 79→81 (horse numbering) and their equivalents are generally described without secondary structure: these are connection elements which also cover the other faces of the heme. The sequence alignment of Figure 8 can also be analyzed in view of the heme ring current shift effect on nearby residues. The $C^{\beta}H_3$ of Ala 22 in $c_{553}$ exhibits an usual chemical shift of –0.88 ppm, and similarly, one of the $C^{\alpha}H$ of Gly 24 in $c_{551}$ lies at –0.03 ppm. This observation supports a similar location of these two residues with respect to the heme group (Schulman et al., 1970). A second example of an NMR-supported alignment is given by Gly 51 of $c_{553}$ ($\delta_{NH}$ = 10.39) and Val 55 of $c_{551}$ ($\delta_{NH}$ = 10.45).

In conclusion, the structural arguments on horse cytochrome *c* and cytochromes $c_{551}$ from *P. aeruginosa* (Detlefsen et al., 1990, 1991) and $c_{553}$ from *D. vulgaris* Hildenborough confirm with almost no major modification the sequence alignment originally proposed by Dickerson (1980). However, our sequence alignment (Figure 8) significantly differs from that published along the X-ray data on *D. vulgaris* Miyazaki (Nakagawa et al., 1990), although both the NMR and crystallographic data are at first glance similar and consistent.

Without resorting to molecular modeling, the topology of the 3D structure of cytochrome $c_{553}$ as well as the aromatic ring mobility have been analyzed in detail in this paper. These data pave the way for the NMR-based structure refinement and for the investigation of the conformation of the oxidized state, both in progress in our laboratory.

## ACKNOWLEDGMENT

Dr. Mireille Bruschi is gratefully acknowledged for her continuous support during this project and Dr. Michael Caffrey for helpful discussions on cytochromes. We thank Dennis Hare (Hare Research, Inc., Bothell, WA) for providing us with a free copy of his software Felix 2.0 for 2D and 3D NMR processing.

## REFERENCES

Bertrand, P., Bruschi, M., Denis, M., Gayda, J.-P., & Manca, F. (1982) *Biochem. Biophys. Res. Commun. 106*, 756–760.
Bianco, P., Haladjian, J., Loufti, M., & Bruschi, M. (1983) *Biochem. Biophys. Res. Commun. 113*, 526–530.
Cai, M. L., & Timkovich, R. (1991) *Biochem. Biophys. Res. Commun. 178*, 309–314.
Chau, M.-H., Cai, M. L., & Timkovich, R. (1990) *Biochemistry 29*, 5076–5087.
Chothia, C., & Lesk, A. M. (1985) *J. Mol. Biol. 182*, 151–158.
Davis, D. G., & Bax, A. (1985) *J. Am. Chem. Soc. 107*, 2820–2821.
Dayhoff, M. O., & Barker, W. C. (1976) in *Atlas of Protein Sequence and Structure* (Dayhoff, M. O., Ed.) Vol. 5, pp 25–49, National Biomedical Research Foundation, Washington, DC.
Detlefsen, D. J., Thanabal, V., Pecoraro, V. L., & Wagner, G. (1990) *Biochemistry 29*, 9377–9386.
Detlefsen, D. J., Thanabal, V., Pecoraro, V. L., & Wagner, G. (1991) *Biochemistry 30*, 9040–9046.
Dickerson, R. E. (1980) *Sci. Am. 242*, 99–110.
Dickerson, R. E., & Timkovich, R. (1975) in *The Enzymes* (Boyer, P. O., Ed.) pp 397–547, Academic Press, New York.
Feng, Y., Roder, H., Englander, S. W., Wand, A. J., & DiStefano, D. L. (1989) *Biochemistry 28*, 195–203.
Freeman, R., Friedrich, J., & Wu, X.-L. (1988) *J. Magn. Reson. 79*, 561–567.
Gao, Y., Boyd, J., Pielak, G. J., & Williams, R. J. P. (1991) *Biochemistry 30*, 7033–7040.
Griesinger, C., Otting, G., Wüthrich, K., & Ernst, R. R. (1988) *J. Am. Chem. Soc. 110*, 7870–7872.
Le Gall, J., & Bruschi-Heriaud, M. (1968) in *Structure and Function of Cytochromes* (Okunuki, K., Kamen., M. D., & Sekuzu, J., Eds) pp 467–470, University of Tokyo Press, Tokyo.
Macura, S., Huang, Y., Suter, D., & Ernst, R. R. (1981) *J. Magn. Reson. 43*, 259–281.
Mathews, F. S. (1985) *Prog. Biophys. Mol. Biol. 145*, 1–56.
Nakagawa, A., Nagashima, E., Higushi, Y., Kusunocki, M., Matsuura, Y., Yasuoka, N., Katsube, Y., Chichara, H., & Yagi, Y., (1986) *J. Biochem. 99*, 605–606.
Nakagawa, A., Higuchi, Y., Yasuoka, N., Katsube, Y., & Yagi T. (1990) *J. Biochem. 108*, 701–703.
Ogata, M., Akira, K., & Yagi, T. (1981) *J. Biochem. 89*, 1423–1431.
Oh, B.-H., & Markley, J. L. (1990) *Biochemistry 29*, 3993–4004.
Plateau, P., & Guéron, M. (1982) *J. Am. Chem. Soc. 104*, 7310–7311.
Rance, M., Sørensen, O. W., Bodenhausen, G., Wagner, G., Ernst, R. R., & Wüthrich, K. (1983) *Biochem. Biophys. Res. Commun. 117*, 479–485.
Schulman, R. G., Wüthrich, K., Yamane, T., Patel, D. J., & Blumberg, W. E. (1970) *J. Mol. Biol. 53*, 143–157.
Senn, H., & Wüthrich, K. (1985) *Q. Rev. Biophys. 18*, 111–134.
Senn, H., Guerlesquin, F., Bruschi, M., & Wüthrich, K. (1983) *Biochim. Biophys. Acta 748*, 194–204.
Simorre, J.-P., & Marion, D. (1991) *J. Magn. Reson. 94*, 426–432.
States, D. J., Haberkorn, R. A., & Ruben, D. J. (1982) *J. Magn. Reson. 48*, 286–292.
Takano, T., & Dickerson, R. E. (1981) *J. Mol. Biol. 153*, 79–94.
van Rooijen, G. J. H, Bruschi, M., & Voordouw, G. (1989) *J. Bacteriol. 171*, 3575–3578.
Wagner, G., DeMarco, A., & Wüthrich, K. (1976) *Biophys. Struct. Mech. 2*, 139–158.
Wüthrich, K. (1986) *NMR of Proteins and Nucleic Acids*, Wiley, New York.
Yagi, T. (1979) *Biochim. Biophys. Acta 548*, 96–105.